Cooling and localization of atoms in laser-induced potential wells

R. Taïeb,* R. Dum, J. I. Cirac,† P. Marte, and P. Zoller
Joint Institute for Laboratory Astrophysics and Department of Physics, University of Colorado, Boulder, Colorado 80309-0440
(Received 9 December 1993)

We discuss theoretically the cooling and localization of atoms in deep potentials induced by a far-off-resonant standing-wave laser. For a two-level atom cooling occurs via a Sisyphus mechanism. For a Λ system we discuss a Raman cooling scheme similar to the one proposed for laser cooling in ion traps.

PACS number(s): 32.80.Pj, 42.50.Ar

I. INTRODUCTION

Laser cooling of neutral atoms is typically accomplished in optical molasses, employing a configuration of counterpropagating laser beams. The role of the laser is twofold: it provides a damping mechanism, and leads to the formation of optical potentials (the ac Stark shift of the atomic ground states). Energies achieved in these experiments can be lower than the depth of the optical potential, so that significant numbers of atoms are trapped and localized in the minima of the wells. Atomic motion in the laser-induced potentials is quantized. Raman transitions between the vibrational levels in the optical potential (band structure) have been observed in recent experiments [1], and have been studied theoretically in Refs. [2,3].

The purpose of this paper is to investigate a configuration for laser cooling and strong atomic localization where two lasers, a "trapping laser" and a "cooling laser," are employed. The role of the trapping laser is to provide "deep" potential wells for the atoms without, however, scattering photons; this is achieved by strongly detuning this laser from the atomic resonances [see Fig. 1(a)]. The depth of the potential will be proportional to the light intensity of this laser. In contrast to a "dipole trap" [4] where a nonresonant running-wave laser is focused down to a few wavelengths, we will study a situation where the trapping laser is a standing-wave configuration (which leads to periodic potential wells on the scale given by the laser wavelength). The purpose of the second laser is to provide cooling of atoms in the optical potential formed by the trapping laser. This laser will be tuned near an atomic resonance transition.

In the simplest case of an atomic transition described by a two-level atom, the ground state $|g\rangle$ and excited state $|e\rangle$ of the atom in the nonresonant standing-wave (SW) light field of the trapping laser $\vec{E}_T(x,t) = \mathcal{E}_T(x)\ \vec{\epsilon}_T e^{-i\omega_T t}+\text{c.c.}$ will experience a position-dependent ac Stark shift,

$$V_i(x) = \alpha_i(\omega_T)\mathcal{E}_T(x)^2 \equiv \alpha_i(\omega_T)\mathcal{E}_T^2 \sin^2(k_T x) \qquad (i = g, e) \quad (1)$$

(see Fig. 1). Here $\alpha_{g,e}(\omega_T)$ is the dynamic atomic polarizability of the atomic ground state (excited state) at the frequency of the trapping laser ω_T; $\mathcal{E}_T(x) = \mathcal{E}_T \sin(k_T x)$ is the position-dependent laser amplitude. The ac Stark shift $V_i(x)$ $(i = g, e)$ provides an optical potential with periodicity of half of the wavelength $\lambda_T/2$ (where $k_T = 2\pi/\lambda_T$) which depends on the internal state of the atom. The corresponding atomic Hamiltonian is

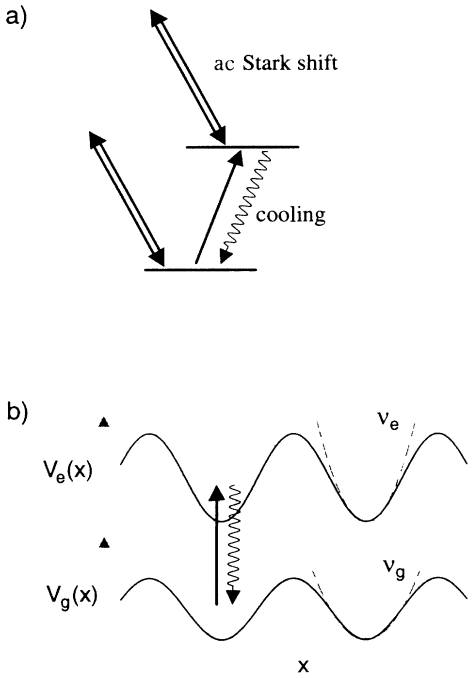

FIG. 1. (a) Dressing and cooling scheme for a two-level system. (b) The laser-induced spatially varying Stark shift of the ground and excited states are plotted for $\nu_e > \nu_g$.

*Present address: Laboratoire de Chimie-Physique Matiere et Rayonnement, 11 rue Pierre et Marie Curie, 75231 Paris Cedex 05, France.

†Permanent address: Departamento de Fisica Aplicada, Facultad de Ciencias Quimicas, Universidad de Castilla-La Mancha, 13071 Ciudad Real, Spain.

$$H_{0A} = \frac{\hat{p}^2}{2M} + \sum_{i=g,e} V_i(\hat{x})|i\rangle\langle i|, \quad (2)$$

where the first term is the kinetic energy of the atom. The depth of the potential is proportional to the laser intensity. We note that, depending on the sign of the atomic polarizabilities $\alpha_i > 0$ (< 0) (i.e., depending on the frequency ω_T), the minima of the potential $V_i(x)$ will be at the nodes (antinodes) of the standing-wave field. Laser cooling by the second laser, which is near resonant with the $|g\rangle - |e\rangle$ transition, will localize the atoms near the potential minima. Thus localization near the nodes of the trapping field has the advantage that light scattering involving the trapping beams (a heating mechanism) will be strongly suppressed.

In the initial stages of the cooling process the atoms will have a homogeneous spatial distribution on the scale of the wavelength of the trapping laser. A typical configuration for the cooling laser would then consist of a pair of counterpropagating light waves (SW) similar to the laser configurations in optical molasses. In contrast, a running wave (RW) would lead to an unbalanced radiation pressure. In the final stages of the cooling process when the atoms are already well localized near the potential minima, the details of the laser configuration (SW vs RW) are unimportant. In our models in Secs. II and III, which describe the final stages of cooling and localization, we will assume for simplicity a RW cooling laser. Quantum Monte Carlo simulations for a SW configuration will be discussed in Sec. IV.

To the extent that the atoms are well localized near the potential minima (Lamb-Dicke limit) we can approximate the potentials by harmonic oscillators,

$$V_i(x) \simeq \alpha_i(\omega_T)\mathcal{E}_T^2 k_T^2 x^2 = \frac{1}{2}M\nu_i^2 x^2 \quad (i = g, e) \quad (3)$$

(assuming $\alpha_i > 0$). The oscillator frequency is

$$\nu_i = \sqrt{2\alpha_i(\omega_T)\,(\mathcal{E}_T k_T)^2/M} \quad (i = g, e) \quad (4)$$

which scales with the square root of the trapping laser intensity. In the harmonic approximation the energy spacing between the vibrational levels is $\hbar\nu_i$, and the width of the ground-state wave function (the optimum achievable atomic localization) is $\delta x^2 = \hbar/(2M\nu_g)$ (assuming that the dominant parts of the atoms are in state $|g\rangle$). We will show below that for alkali atoms the typical localization that can be achieved is on the order of a few percent of the optical wavelength for trapping intensities of a few MW/cm^2 [5].

Laser cooling by a running-wave laser for the two-level system described by the atomic Hamiltonian (2) is reminiscent of laser cooling of trapped ions in the Lamb-Dicke limit, i.e., in the limit where the localization of the atoms (as given by the ground state of the harmonic oscillator potential) is much smaller than the wavelength of the cooling laser [6]. Thus one expects that laser cooling mechanisms known from ion traps, in particular sideband cooling, can be applied to the present configuration. Sideband cooling in an ion trap allows cooling of ions to the vibrational ground state [6,7]. The condition for sideband cooling is that the trap frequency is larger than the radiative linewidth Γ of the atom so that the motional sidebands of the ion in the trap are well resolved (strong-binding limit). Tuning of the cooling laser to the (well-resolved) lower motional sideband then leads to optical pumping to the ground state of the trap. In the case of optical potentials [compare Eq. (1)] the strong-binding limit will be reached for sufficiently high intensities of the trapping laser (typically a few MW/cm^2) [5]. Thus to the extent that the optical potential (1) can be made much deeper than in the usual optical molasses, in the present scheme we expect better localization of the atoms and a larger fraction of atoms in the vibrational ground state. The important difference between laser cooling of neutral atoms in laser-induced potentials (the model studied in this paper) and laser cooling in an ion trap is, however, that for an ion trap the ground and excited state potentials are identical, $\nu_g = \nu_e$, while in the present situation we typically have $\nu_g \neq \nu_e$ due to different dynamic polarizabilities of the states. We will show below that for the model studied in this paper, laser cooling can only be obtained for $\nu_e \geq \nu_g$ ($\nu_e < \nu_g$ leads to heating). For $\nu_e > \nu_g$ we find a novel "Sisyphus cooling" mechanism which produces cooling rates much faster than those known from laser cooling of trapped ions. In addition, for $\nu_e > \nu_g$ a detuning of the laser to the blue side of the atomic transition will be shown to result in accumulation of atoms in a few excited states of the trap, corresponding to preparation of nonclassical states of motion.

The sideband cooling condition for a two-level atom, $\nu_{g,e} > \Gamma$, requires high trapping laser intensities; in the case of ions this condition can only be fulfilled with metastable levels with long radiative lifetimes [6,7]. In the context of ion traps, Raman cooling schemes have been discussed where Raman transitions are induced between two atomic ground states [8], i.e., two ground state levels play the role of the ground state $|g\rangle$ and excited state $|e\rangle$ of the two-level system discussed above, with the optical pumping rate Γ' playing the role of the radiative decay rate Γ. Since the optical pumping time for Raman transitions can be much longer than the radiative lifetime, the sideband cooling condition $\nu_{g,e} > \Gamma'$ is easier to satisfy in this case. A similar Raman scheme can be employed in the present case of laser-induced potentials, inducing, for example, Raman transitions between different Zeeman levels or hyperfine-structure components of the atomic ground state. For alkali atoms the ground states are s states. In this particular case the ac Stark shifts induced by the trapping laser are identical (within a few percent) so that $\nu_g = \nu_e$, and we have a complete analogy to Raman cooling in an ion trap.

The paper is organized as follows. In Sec. II we discuss cooling mechanisms in laser-induced potentials within a two-level model in the harmonic potential approximation. Section III is devoted to Raman cooling. In Sec. IV we compare the results of the harmonic trapping potential approximation with a full quantum Monte Carlo simulation periodic laser potential.

II. TWO-LEVEL SYSTEM

A. The model

We consider a two-level system with ground level $|g\rangle$ and excited level $|e\rangle$ (Fig. 1). The transition frequency is ω_{eg}. The cooling laser light is assumed to have the form of a traveling wave where the positive frequency part of the electric field is given by $\vec{E}_c^{(+)}(x,t) = \mathcal{E}e^{i(kx-\omega t)}\vec{\epsilon}$ with frequency ω, $k = 2\pi/\lambda$ the wave vector with λ the wavelength of the laser light, and $\vec{\epsilon}$ the polarization vector. In this section we discuss a model where the "trapping laser" induced periodic potential (1) is approximated by harmonic oscillator potentials with oscillation frequencies ν_g and ν_e for the ground and excited states, respectively. We expect this to be a good approximation in the final stages of the cooling process when the atomic center-of-mass distribution is well localized on the scale given by the wavelength λ_T (Lamb-Dicke limit), i.e., the dimensionless parameter $\eta_{e,g}$ defined by ($\hbar = 1$)

$$\eta_{e,g}^2 = k^2/(2M\nu_{e,g}) \tag{5}$$

is much smaller than 1. This approximation neglects tunneling between neighboring potential wells and effects near the barrier of the trapping potential. In Sec. IV we will compare the results of the present model with quantum simulation results of the full quantum master equation based on the potential (1) and a standing-wave cooling laser. The atomic Hamiltonian describing the motion in the trapping potential in the presence of a cooling laser is ($\hbar = 1$)

$$\begin{aligned} H_A = &|\, g\,\rangle\langle\, g\,| \left[\frac{p^2}{2m} + \frac{1}{2}m\nu_g^2 x^2\right] \\ &+|\, e\,\rangle\langle\, e\,| \left[\frac{p^2}{2m} + \frac{1}{2}m\nu_e^2 x^2\right] \\ &-\frac{\Delta}{2}(|\, e\,\rangle\langle\, e\,| - |\, g\,\rangle\langle\, g\,|) \\ &+\frac{\Omega}{2}\,(e^{ikx}|\, e\,\rangle\langle\, g\,| + e^{-ikx}|\, g\,\rangle\langle\, e\,|) \end{aligned} \tag{6}$$

with $|i\rangle\langle j|$ atomic projectors, $\Delta = \omega - \omega_{eg}$ the laser-atom detuning, and Ω the Rabi frequency for the cooling laser.

The interaction of the atom with the vacuum modes of the radiation (spontaneous emission) can be described in terms of a master equation,

$$\dot{\rho} = -i(H_{\text{eff}}\rho - \rho H_{\text{eff}}^\dagger) + \mathcal{L}^d\rho \tag{7}$$

with $\rho(t)$ the reduced atomic density operator and $H_{\text{eff}} = H_A - i\Gamma/2|\, e\,\rangle\langle\, e\,|$ an effective non-Hermitian Hamiltonian which includes the radiative damping. The term

$$\mathcal{L}^d\rho = \frac{\Gamma}{2}\int_{-1}^{1} du N(u)|\, g\,\rangle\langle\, e\,|e^{-iku\hat{x}}\,\rho\, e^{iku\hat{x}}|\, e\,\rangle\langle\, g\,| \tag{8}$$

describes the return of the atomic electron to the ground state with each photon emission, including the associated momentum transfer; $N(u) = 3(1+u^2)/8$ is the angular distribution of the emitted light [9].

In the following subsections we discuss the quantum master equation with adiabatic elimination of the excited state, a semiclassical picture of the Sisyphus cooling mechanism [10] in the optical potential with $\nu_g \neq \nu_e$, and the numerical results.

B. Quantum master equation: Adiabatic elimination of the excited state

For a solution of the quantum master equation (7) it is convenient to work in a mixed basis of harmonic oscillator eigenstates $|n\rangle_g$ of the ground state potential, and $|n\rangle_e$ for the excited states ($n = 0, 1, \ldots$). These states are defined by

$$a_i^\dagger a_i |n\rangle_i = n|n\rangle_i \quad (i = g, e), \tag{9}$$

where $a_g^\dagger$ and a_g are raising and lowering operator for the ground state harmonic oscillator (frequency ν_g), and $a_e^\dagger$ and a_e are the corresponding operators for the excited state (frequency ν_e). The two sets of operators $a_{g,e}^\dagger$, $a_{g,e}$, and the eigenstates $|n\rangle_{g,e}$ are related by a Bogoliubov transform (see Appendix A).

The dipole coupling between the ground state and excited state involves matrix elements of the form

$${}_e\langle m|e^{ik\hat{x}}|n\rangle_g = {}_e\langle m|n\rangle_g + i\,{}_e\langle m|k\hat{x}|n\rangle_g + \cdots . \tag{10}$$

The operator $\exp(ik\hat{x})$ describes the momentum transfer associated with the transition. In the Lamb-Dicke limit the exponential can be expanded. The first, second, etc. terms on the right-hand side (RHS) of Eq. (10) correspond to terms that are zero, first, etc., order in the small Lamb-Dicke parameter $\eta \ll 1$. For an ion trap we have $\nu_g = \nu_e$ and thus $|n\rangle_g = |n\rangle_e$, so that the first term on the RHS of (10) is a Kronecker delta $\delta_{m,n}$, and only the higher order Lamb-Dicke terms will couple states with different motional quantum numbers $n \neq m$. As a consequence, for an ion trap there is no cooling in zeroth order in the Lamb-Dicke parameter; the cooling rate is proportional to η^2, and is thus much slower than the time scale of the internal transition (Γ) which is the basis for the adiabatic elimination scheme employed in Ref. [6].

In the present case ($\nu_g \neq \nu_e$) there is a zeroth-order coupling (overlap) between the even (odd) states (${}_e\langle m|n\rangle_g \neq 0$ for $n = m, m \pm 2, \ldots$), while matrix elements connecting the even to the odd oscillator states are smaller by a factor η. Thus in the master equation the even (odd) states are coupled by rates comparable to the time scale of the internal atomic transition rates ($\sim 1/\Gamma$), while the coupling between even and odd states occurs on a time scale of order $\eta^2\Gamma$. This fast time scale of cooling (in order η^0) is related to the (induced) Sisyphus cooling mechanism discussed in Sec. II C and does not exist in this form in ordinary ion traps.

In order to find the steady state solution of master equation (7) one can use a truncated basis of Fock states. In Fig. 2 we have plotted the final energy of the atom as a function of the Rabi frequency for $\nu_g = 3\Gamma$, $\nu_e = 6\Gamma$,

and $\Delta = -5\Gamma$. Note that the lowest energies are found for small Rabi frequencies, i.e., for low intensities. In this case the saturation parameter $s = \Omega^2/2(\Delta^2+\Gamma^2/4) \ll 1$, and therefore the excitation rate from the ground to the excited state ($\sim s\Gamma$) is much smaller than the spontaneous transition rate Γ. This allows us to eliminate the excited state adiabatically. Furthermore, we assume that the excitation rate is slow on the time scale of oscillations $s\Gamma \ll \nu_{g,e}$ which allows a secular approximation by decoupling trap coherences from trap population terms [11]. The result is a rate equation for the populations $\Pi_n = {}_g\langle n|\langle g|\rho(t)|g\rangle|n\rangle_g$,

$$\dot{\Pi}_n = -\frac{\Omega^2\Gamma}{4}\left(\sum_m \frac{\left|\,{}_e\langle m\mid e^{ikx}\mid n\,\rangle_g\,\right|^2}{(E_{m_e}-E_{n_g}-\Delta)^2+\frac{\Gamma^2}{4}}\right)\Pi_n + \frac{\Omega^2\Gamma}{4}\int_{-1}^{+1} du\, N(u)\sum_l \left|\sum_m \frac{{}_g\langle n\mid e^{-ikux}\mid m\,\rangle_e\langle m\mid e^{ikx}\mid l\,\rangle_g}{(E_{m_e}-E_{l_g}-\Delta)-i\frac{\Gamma}{2}}\right|^2 \Pi_l\ .$$

The first term on the RHS of this equation is a loss term for level $|g\rangle|n\rangle_g$ due to transitions to states $|g\rangle|m\rangle_g$ while the second term describes the population transfer $|g\rangle|l\rangle_g \rightarrow |g\rangle|n\rangle_g$ by absorption of a laser photon ($|g\rangle|l\rangle_g \rightarrow |e\rangle|m\rangle_e$) followed by a spontaneous emission where a photon is emitted in the direction $u = \cos\Theta$. In writing this equation we have not (yet) explicitly performed the Lamb-Dicke expansion although the assumption of a harmonic trapping potential implies this approximation.

Figure 3 shows results for the trap populations Π_n and the corresponding spatial distribution $P(x) = \langle x|\langle g|\rho(t)|g\rangle|x\rangle$ which were obtained by numerical solution of the rate equation (11). We note that for low intensities the steady state is independent of the Rabi frequency of the exciting laser. The trap frequencies in Fig. 3 are $\nu_g = 1.5\Gamma$, $\nu_e = 3\Gamma$. For $\Delta = -4\Gamma < 0$ (red detunings) we find that the populations obey approximately a Maxwell-Boltzmann distribution [Fig. 3(a)]. In the limit $\nu_e > \nu_g > \Gamma$ practically all of the population is in the trap ground state. This situation is reminiscent of sideband cooling in ion traps, where the atom is in the state $|n=0\rangle|g\rangle$ and can no longer be excited [6]. In our case this corresponds to laser detunings $\Delta \sim -\nu_g, -\nu_e$. The spatial distribution in this case is a Gaussian [Fig. 3(b), solid line] with x_0 the size of the ground state. For $\Delta = \Gamma$ (blue detuning) we

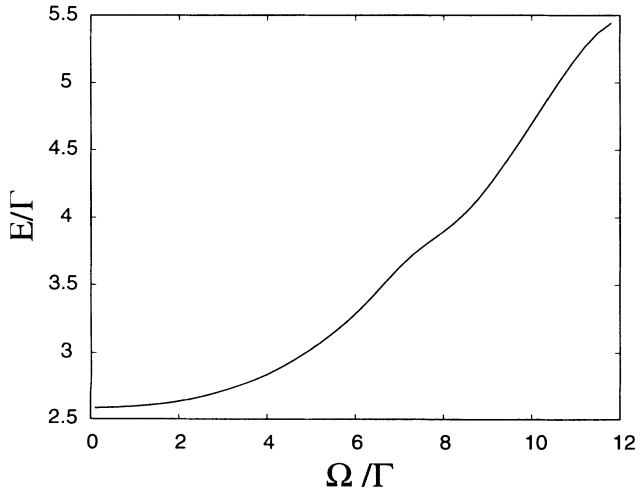

FIG. 2. Final energy as a function of the Rabi frequency obtained by solving numerically the full master equation. Parameters are $\nu_g = 3\Gamma$, $\nu_e = 6\Gamma$, and $\Delta = -5\Gamma$.

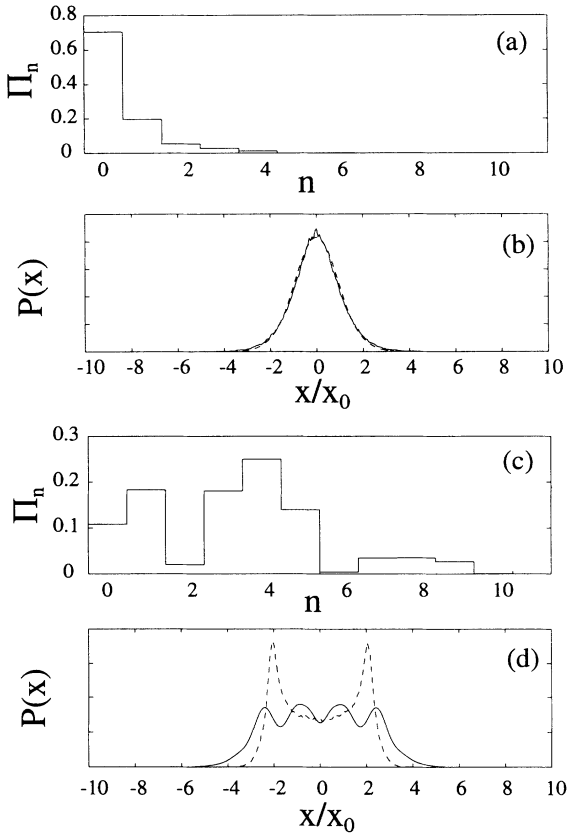

FIG. 3. Population Π_n of the oscillator levels of the ground state (a),(c) and position distribution (b),(d) for $\Delta = -4\Gamma$ (a),(b) and $\Delta = 4\Gamma$ (c),(d) and $\nu_e = 3\Gamma$, $\nu_g = 1.5\Gamma$. The scale of position is in units of $x_0 = \delta x(n=0)$ (the ground state of the harmonic oscillator in state $|g\rangle$). Dashed lines in (b) and (d) are the semiclassical result obtained by simulating the rate equations given in Sec. II C.

have heating for the low-lying trap states and cooling for the higher-lying states (see also the Sisyphus picture described in Sec. II C). This is reflected in the non-Maxwell-Boltzmann distribution of Fig. 3(c). We see that the corresponding spatial distribution [Fig. 3(d), solid line] has a multipeaked structure that reflects the spatial distribution of excited harmonic oscillator eigenfunctions. These oscillations are not present in the spatial distributions obtained in a semiclassical approximation (cf. Sec. II C) and thus represent quantum features ("preparation of nonclassical states of motion"). By modifying the parameters one can obtain a distribution that is sharply peaked at a certain n quantum number and in this sense prepare an approximate (excited) Fock state of motion $|n\rangle$ $(n > 0)$.

Red laser detunings and low Rabi frequencies lead to the lowest temperatures and thus optimum localization of the atoms in the potential wells, while larger Rabi frequencies lead to a faster cooling rate (for a discussion of the intensity dependence refer to Sec. II C). In terms of oscillator eigenfunctions an estimate of the localization is given by

$$\delta x^2 = \frac{\hbar}{m\nu_g}(\langle n\rangle + \tfrac{1}{2}). \tag{11}$$

The ground state as a minimum-uncertainty state gives a lower bound to the possible localization. For alkali atoms and trap frequencies ν_g of the order of Γ, the localization results in about 1% of the optical wavelength. Finally, we wish to stress the fact that δx^2 is inversely proportional to the square root of the trapping laser intensity.

C. Semiclassical treatment: Sisyphus cooling

In contrast to the well-known cooling mechanisms in ion traps (see the Introduction), the fact that the trap frequencies of the ground and excited state are different leads to a new type of cooling, similar to Sisyphus cooling of atoms in a standing light wave [10]. This mechanism does not depend on the momentum exchange due to photon recoil. We describe qualitatively this cooling mechanism from the semiclassical point of view, where the position and momentum of the atom are described as classical variables.

The Hamiltonian part of the interaction neglecting photon recoil [i.e., in zeroth order in η as given in Eq. (5)] is

$$H = \frac{p^2}{2m} + \frac{1}{2}m\nu_m^2 x^2 - \frac{\Delta'(x)}{2}(|\,e\,\rangle\langle\,e\,| - |\,g\,\rangle\langle\,g\,|) + \frac{\Omega}{2}(|\,e\,\rangle\langle\,g\,| + |\,g\,\rangle\langle\,e\,|). \tag{12}$$

Here, we have defined an average trap frequency

$$\nu_m^2 = \frac{\nu_e^2 + \nu_g^2}{2} \tag{13}$$

and a position-dependent detuning

$$\Delta'(x) = \Delta - \frac{1}{2}m(\nu_e^2 - \nu_g^2)x^2 \tag{14}$$

resulting from the different oscillation frequencies for the ground and excited state [see Fig. 1(b)]. The situation described by the Hamiltonian (12) is reminiscent of the well-known Sisyphus-type cooling in optical molasses, where the spatial dependence of the Rabi frequency provides an effective potential in which the atom is cooled [10]. In the present situation, however, this familiar spatial dependence of the Rabi frequency is replaced by a position dependence of the detuning. In order to give a physical picture of this cooling mechanism, we use the same approach as that for optical molasses. We first diagonalize the Hamiltonian (12) using the dressed atom basis,

$$|+\rangle = \sin\theta(x)|g\rangle + \cos\theta(x)|e\rangle, \tag{15}$$

$$|-\rangle = \cos\theta(x)|g\rangle - \sin\theta(x)|e\rangle, \tag{16}$$

with

$$\operatorname{cotan}2\theta(x) = -\frac{\Delta'(x)}{\Omega} \quad \left(0 \le \theta \le \frac{\pi}{2}\right). \tag{17}$$

In this basis, the Hamiltonian can be written as

$$H = \left[\frac{p^2}{2m} + V_+(x)\right]|+\rangle\langle+| + \left[\frac{p^2}{2m} + V_-(x)\right]|-\rangle\langle-| \tag{18}$$

where the dressed-state-dependent potentials are

$$V_\pm = \frac{1}{2}m\nu_m^2 x^2 \pm \frac{1}{2}\sqrt{\Delta'(x)^2 + \Omega^2}. \tag{19}$$

The dressed state picture is particularly suited for situations in which $\sqrt{\Delta'(x)^2 + \Omega^2} \gg \Gamma$. In this case, one can perform a secular approximation in the equations for the dressed-state populations Π_+ and Π_-, obtaining

$$\frac{d\Pi_\pm}{dt} = -\Gamma_{\pm,\mp}(x)\Pi_\pm + \Gamma_{\mp,\pm}(x)\Pi_\mp \pm v\frac{d\theta(x)}{dx}(\rho_{+,-} + \rho_{-,+}). \tag{20}$$

Here

$$\Gamma_{+,-}(x) = \Gamma\cos^4[\theta(x)], \quad \Gamma_{-,+}(x) = \Gamma\sin^4[\theta(x)] \tag{21}$$

are the transition rates due to spontaneous emission between dressed levels, and v is the velocity of the atom. The last term in Eq. (20) expresses the possible modification of the dressed-state populations due to the spatial variation of the dressed levels, and is usually termed nonadiabatic kinetic coupling since it describes the possibility of changing from one dressed state to the other in the absence of spontaneous emission. As in the case of a free particle, and for the qualitative picture given in this section, we omit the nonadiabatic kinetic coupling in the evolution equations of the dressed-state populations

(the validity of this assumption is discussed in Appendix B). Hence, we finally get a rate equation for transitions of the atom between different state-dependent potentials (bipotential motion).

We have plotted in Figs. 4 and 5 the trapping potentials $V_{\pm}$, as well as the transition rates as a function of the position for $\nu_e > \nu_g$ and two situations of interest: $\Delta < 0$ (Fig. 4) and $\Delta > 0$ (Fig. 5). From these figures the cooling process can be explained as follows. In the first case ($\Delta < 0$), when the atom is in the state $|-\rangle$ it is preferably transferred to the state $|+\rangle$ when it is close to the position $x \approx 0$, since the transition rate $\Gamma_{-,+}$ is maximum at this point (note that it is precisely at $x = 0$ where the state $|-\rangle$ is more "contaminated" by the internal excited state $|e\rangle$). On the other hand, once the atom is in $|+\rangle$ it is preferentially transferred to $|-\rangle$ for $|x| > 0$, since $\Gamma_{+,-}$ is an increasing function of x^2. As can be seen from Fig. 4, in a cycle $|-\rangle \rightarrow |+\rangle \rightarrow |-\rangle$ the atomic energy decreases, and therefore the atom is cooled very efficiently. This is analogous to the well-known Sisyphus mechanism found in polarization gradient cooling [10]. In the case $\Delta > 0$, and if the ion is oscillating with high energy, the same argument applies. However, at the end of the process (low energies), when the amplitudes of the oscillations are close to the avoided crossing between the two potentials, the situation is reversed: now the atom climbs a less steep potential hill when it is in $|+\rangle$ rather than when it is in $|-\rangle$, and therefore the atom tends to heat up. Consequently, the atom tends to oscillate with the amplitude corresponding to the position of anticrossing of the two potentials. We note that this is what also results from the quantum calculation Sec. II B [see Fig. 3(d)]. However, the wiggles appearing in the figure cannot be explained within this semiclassical picture; they reflect the node structure of the quantum mechanical wave functions of the harmonic oscillator states.

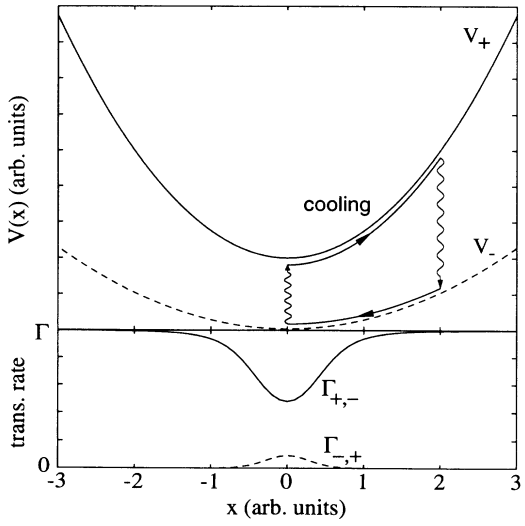

FIG. 4. Dressed state potentials (upper panel) and transition rates (lower panel) as a function of position for $\nu_e > \nu_g$ and a red detuning ($\Delta < 0$). The solid (dashed) lines correspond to the potential of state $|+\rangle(|-\rangle)$ and the transition rates $\Gamma_{+,-}$ ($\Gamma_{-,+}$), respectively.

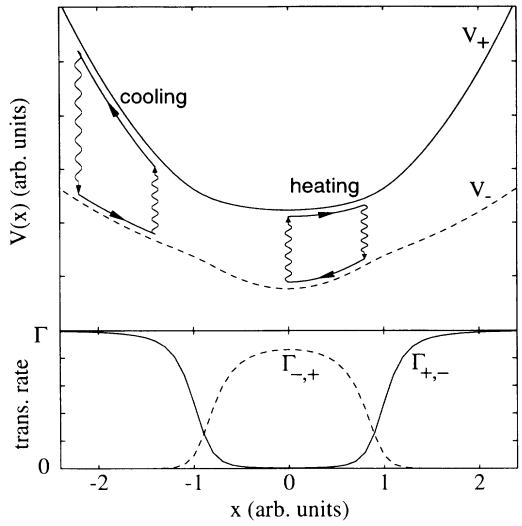

FIG. 5. Same as Fig. 4 with a blue detuned laser ($\Delta > 0$).

Using similar arguments one can show that cooling is not possible for $\nu_g > \nu_e$, since for sufficiently high energies the potential $V_-(x) > V_+(x)$ $(x \rightarrow \infty)$ and therefore the transitions from $|+\rangle \rightarrow |-\rangle$ also increase the energy of the atom.

Following Ref. [15], we have performed Monte Carlo simulations of the rate equations (20). Results are plotted in Figs. 3(b) and 3(d). Note that in the red detuning case, the result is basically the same as that obtained with a quantum calculation. In contrast, for positive detunings, the quantum calculation displays wiggles in the position distribution, which are absent with the semiclassical model.

We wish to stress the fact that this cooling mechanism does not depend on the transfer of the recoil energy due to atomic transitions, and therefore the cooling can be very efficient provided transitions between the dressed states take place very rapidly. The above qualitative picture permits an estimate of the cooling time (see Appendix B). As shown in the Appendix, in the low excitation limit $\Omega < |\Delta|$ the cooling rate is proportional

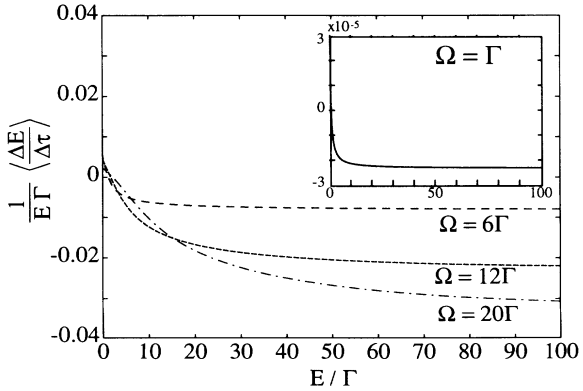

FIG. 6. Cooling rate in a semiclassical approximation as a function of energy for $\nu_e = 6\Gamma$, $\nu_g = 3\Gamma$, and $\Delta = -5\Gamma$. The different curves correspond to changing Rabi frequencies. The inset shows the cooling rate for $\Omega = \Gamma$ on a different scale.

to the fourth power of the Rabi frequency, and therefore the larger the Rabi frequency, the more efficient the cooling results. In Fig. 6 we have plotted the cooling rate given by (B3) of Appendix B as a function of the energy E [as given in Eq. (18)] for different values of the Rabi frequency. At high energies the cooling is faster and increases with the Rabi frequency. Note that for $\Omega \sim \Gamma < |\Delta|$ the cooling rate is very small (inset of Fig. 6). However, for $\Omega \sim |\Delta| \sim 5\Gamma$ the cooling rate increases dramatically. For higher Rabi frequencies, the cooling is faster, but, as we have discussed in Sec. II B, the final energy increases. We note that these results for the cooling time are based on the neglecting of the nonadiabatic kinetic coupling. We have verified these results by comparing semiclassical simulations according to (20) with full quantum simulations performed in Sec. IV.

III. RAMAN COOLING

For a two-level system, cooling to the vibrational ground state of the optical potential is obtained in the strong-binding limit $\nu_e \geq \nu_g > \Gamma$. For alkali atoms this typically requires trapping laser intensities of the order of a few MW/cm^2 [5], or higher. In the context of laser cooling of trapped ions it has been suggested that we reach the sideband cooling limit in a three-level system where two counterpropagating lasers induce Raman transitions between two atomic ground states $|1\rangle$ and $|3\rangle$ (see Fig. 7) [8]. If one of the lasers, say the laser coupling the $1-2$ transition, is much stronger than the laser on the $2-3$ transition, optical pumping will accumulate atoms predominantly in level $|3\rangle$. Thus for low laser intensities and near-resonant Raman detunings the two ground states form an effective two-level system $|g\rangle \equiv |3\rangle$, $|e\rangle \equiv |1\rangle$ with the optical pumping rate $|1\rangle \rightarrow |3\rangle$ playing a role similar to a spontaneous decay constant in the two-level atom. Sideband cooling is obtained when the trap frequency is larger than the optical pumping rate, a condition which is easily satisfied for low laser intensities.

In the typical case of alkali atoms, the two ground states $|1\rangle$ and $|3\rangle$ will be Zeeman states in the manifold of ground s-state hyperfine levels. In this case the ac Stark shift and the trapping potential is *independent* of the magnetic quantum number [4,12]. Thus the oscillation frequencies of the two states are identical and we have a complete analogy to an ion trap.

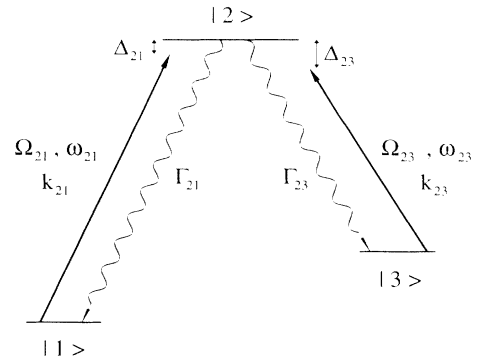

FIG. 7. Level scheme and notations for Raman cooling in a Λ-system.

A. The model: Three-level Λ system

We consider a three-level system interacting with two counterpropagating laser beams. The level configuration and the notation are shown in Fig. 7. The master equation for such a system has the form of Eq. (7) where

$$H_{\text{eff}} = \frac{\hat{p}^2}{2M} + \sum_{\alpha=1,3} [V_\alpha(\hat{x}) + \Delta_{2\alpha}] \,|\, \alpha \,\rangle\langle\, \alpha \,| + \left(V_2(\hat{x}) - i\frac{\Gamma}{2}\right) |\, 2 \,\rangle\langle\, 2 \,| + \sum_{\alpha=1,3} \frac{\Omega_{2\alpha}}{2} \left(e^{ik_{2\alpha}x} |\, 2 \,\rangle\langle\, \alpha \,| + \text{H.c}\right) \tag{22}$$

and

$$\mathcal{L}_d\rho = \Gamma \sum_{\alpha=1,3} \int_{-k}^{+k} du N_\alpha(u) [e^{-iu\hat{z}} |\, \alpha \,\rangle\langle\, 2 \,|] \times \rho \,[|\, 2 \,\rangle\langle\, \alpha \,| \, e^{+iu\hat{z}}] \tag{23}$$

with $N_\alpha(u)$ angular distributions and $\Delta_{2\alpha} = \omega_{2\alpha} - (\omega_2 - \omega_\alpha)$ detunings ($\alpha = 1, 3$). We take the laser wave vectors $|k_{21}| \approx |k_{23}| \approx k$ and assume a symmetric decay $\Gamma_{23} = \Gamma_{21} \equiv \Gamma/2$.

We study in the following a configuration where the trapping potentials of the two ground states are identical, $V_1(x) = V_2(x)$. As noted before, this is realized to a good approximation when the levels $|1\rangle$, $|3\rangle$ are Zeeman hyperfine structure states with zero orbital angular momentum (s states) [12]. Furthermore, we assume the validity of the harmonic approximation (3) for the trapping potentials (oscillator frequencies $\nu_1 = \nu_3 \equiv \nu$, ν_2). In the limit of identical trap frequencies, $\nu_i = \nu$ for all $i = 1, 2, 3$, this model is equivalent to the model of Raman cooling in ion traps studied by Lindberg and Javanainen [8].

B. Reduction to an effective two-level system

For low intensities and large detunings from the excited state

$$\Omega_{23}, \Omega_{21}, \Gamma, \nu_2 \ll \Delta_{21} \approx \Delta_{23} \equiv \Delta \tag{24}$$

and two-photon detunings not too far from the Raman resonance, $|\Delta_{21} - \Delta_{23}| \lesssim \pm\nu$, we can adiabatically eliminate the excited state and reduce the three-level system to an effective two-level atom $\{|1\rangle, |3\rangle\}$. The master equation again has the form (7) with

$$H_{\text{eff}} = \frac{\hat{p}^2}{2m} + \frac{1}{2}m\nu^2\hat{x}^2 - \left(\delta + i\frac{\gamma}{2}\right)\hat{P}_{11} - i\frac{\Omega_{23}^2}{2\Delta^2}\frac{\Gamma}{4}\hat{P}_{33} + \frac{\Omega_0}{2}(\hat{P}_{13}e^{-i\tilde{k}\cdot\hat{x}} + \text{H.c.}) \tag{25}$$

and

$$\mathcal{L}^d\rho = \frac{\Gamma}{2}\sum_{\alpha,\beta=1,3}\frac{\Omega_{2\alpha}^2}{2\Delta^2}\hat{P}_{\beta\alpha}\int_{-1}^{1}duN_\alpha(u)e^{-i(u\cdot k+k_{2\alpha})\cdot\hat{x}} \times\rho e^{i(u\cdot k+k_{2\alpha})\cdot\hat{x}}\hat{P}_{\alpha\beta}. \quad (26)$$

In these equations we have $\Omega_0 = \Omega_{23}\Omega_{21}/(4\Delta)$ the two-photon Rabi frequency,

$$\gamma = \Omega_{21}^2\Gamma/(4\Delta^2) \quad (27)$$

the pumping rate from level 1 to level 3, and

$$\delta = \Delta_{23} - \Delta_{21} - \Omega_{21}^2/(4\Delta) \quad (28)$$

is the Raman detuning containing the Stark shift due to the cooling lasers. Note that $k = k_{21} - k_{23}$, the effective two-photon wave vector, is nonzero only for two counterpropagating laser beams. Identical equations are obtained in this limit for Raman cooling of a trapped ion (since ν_2 no longer enters into the equations).

We take the limit $\Omega_{21} \gg \Omega_{23}$ which results in a population asymmetry $\Pi_1 \ll \Pi_3$ and therefore in an enhancement of transitions $1 \to 3$ over the reverse process. The state $|1\rangle$ corresponds now to the weakly populated "excited state," whereas $|3\rangle$ is the "ground state" of the two-level atom with the two-photon pumping rate γ ($\ll \Gamma$) playing the role of a spontaneous rate. Thus for $\nu \gg \gamma$ we expect a sideband cooling when the Raman transition is tuned to $\delta = \nu$.

Following the standard theory of laser cooling of trapped two-level ions [6,13] in the present problem we obtain rate equations for the populations Π_n in the oscillator basis,

$$\frac{d}{dt}\Pi_n = (n+1)A_-\Pi_{n+1} - [(n+1)A_+ + nA_-]\Pi_n + nA_+\Pi_{n-1} \quad (29)$$

with $A_\pm$ transition rates $n \to n \pm 1$ due to absorption of a photon and subsequent spontaneous emission. In the steady state the populations obey the Bose-Einstein distribution $\Pi_n = (1-q)q^n$ with

$$q = A_+/A_- \quad (q < 1) \quad (30)$$

the ratio between upward and downward transitions, and the total energy is

$$E_{\rm tot} = \hbar\nu\left(\sum_n n\Pi_n + 1/2\right) = \hbar\nu\left(\frac{q}{1-q} + 1/2\right). \quad (31)$$

To calculate the rates $A_\pm$ we followed the theory developed in Ref. [13]. Results of these calculations are discussed in Sec. III C.

C. Discussion

According to Eq. (31) cooling is achieved for $q < 1$. The parameter q measures the ratio between the upward and downward transitions. In Fig. 8 we show the ratio q as a function of the detuning Δ_{21} of the strong laser for a fixed detuning Δ_{23} of the weak laser. We choose $\Delta_{23} = -10\Gamma, \nu = \Gamma/10, \Omega_{23} = 3\times10^{-3}\Gamma$, and $\Omega_{21} = 0.3\Gamma$. The dips (peaks) in this plot correspond to two-photon resonances of transitions $|3\rangle \to |1\rangle$ and $n \to n, n\pm1$. This corresponds to choosing the effective detuning near the lower motional sidebands ($\delta = 0, \pm\nu$). The Raman cooling resonance is given by the usual sideband cooling condition $\delta = -\nu$ and the width of these narrow resonances are given by the optical pumping rate γ. We emphasize that the Stark shift is much larger than the width given by the pumping rate and consequently cannot be neglected.

The inset in Fig. 8 shows the influence of a variation of the oscillation frequency of the state $|2\rangle$ which is neglected in the adiabatic elimination discussed in Sec. III B. From the inset we see that changing ν_2 affects the shape but not the position of the Raman resonance.

In Fig. 9 we compare the cooling rate $W = A_- - A_+$ obtained within the adiabatic approximation (solid line) and the one from a standard ion trap, keeping in the theoretical formulation the excited state (dashed line) for the parameters of Fig. 8. The shift between the two curves corresponds to neglecting the Doppler shift (of the order of the trap frequency ν_2) in the excited state in the adiabatic elimination. The Raman cooling scheme allows cooling of almost all of the population into the ground state for experimentally more favorable conditions than the two-level scheme presented before, i.e., the sideband cooling condition $\nu \gg \Gamma$ is replaced by the much less restrictive inequality $\nu \gg \gamma$. We note, however, that in the Raman system the cooling rate is significantly slower than for the Sisyphus cooling discussed in Sec. II C for the two-level system.

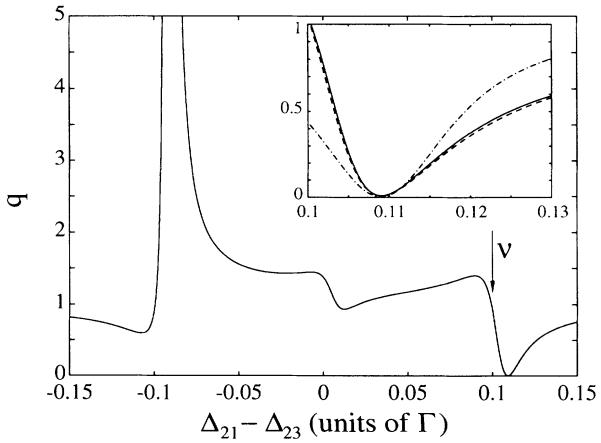

FIG. 8. The ratio q of the transition rates $A_\pm$ as a function $\Delta_{21} - \Delta_{23}$. The transition rates $A_\pm$ as a function Δ_{21}. The parameters are $\nu = \Gamma/10$, $\Delta_{23} = -10\Gamma$, $\Omega_{21} = 0.3\Gamma$, and $\Omega_{21}/\Omega_{23} = 100$. The inset shows the parameter q for a Λ-system where $\nu_2 = \nu_1/2$ (solid line), $\nu_2 = 2\nu_1$ (dashed line), and $\nu_2 = \nu_1$ (dot-dashed line).

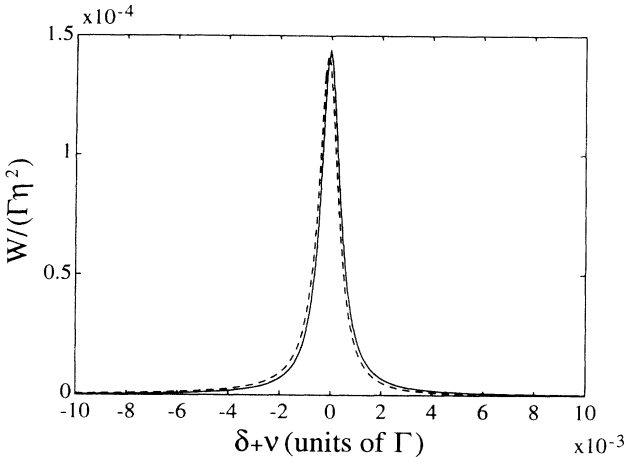

FIG. 9. Cooling rate W as a function of $\delta - \nu$ for the same parameters as in Fig. 8. The solid line corresponds to the approximate result of Sec. III B, the dashed line is the result of a full calculation for $\nu_2 = \nu_1$.

IV. QUANTUM MONTE CARLO SIMULATIONS

In this section we discuss results from quantum Monte Carlo simulations for (i) the initial stages of the cooling process of a two-level atom in a SW configuration for the cooling laser, and (ii) Raman cooling in an $F = 2$ to $F' = 2$ hyperfine structure transition with counterpropagating $\sigma_\pm$ waves.

The models developed in Sec. III are based on a harmonic oscillator approximation for the trapping potential and a RW configuration for the cooling laser. These approximations are valid in the final stages of the cooling process when the atoms are already well localized. For atoms initially close to or above the potential barrier of the trapping potential, a RW would push the atoms out of the interaction region due to the unbalanced radiation pressure. In the final stages of cooling, on the other hand, i.e., with the atoms already near the bottom of the trapping potential, the trapping potential keeps the atoms from escaping (analogous to an ion trap). To study cooling near the barrier we must choose a SW laser configuration. We emphasize that the conclusions of the previous sections remain valid for SW cooling lasers.

Our model assumes a two-level system in the anharmonic potential (1) and in the presence of a SW laser which is near resonant with the transition $|g\rangle - |e\rangle$. To solve the resulting master equations we used the technique of Monte Carlo wave function simulations in the form given in Refs. [14,15]. For a SW cooling laser there are now two different spatial periods in our model, the first related to the wavelength of the cooling laser and the second given by the wavelength of the far-off-resonant laser. For simplicity we have neglected this double periodicity. For the initial condition we take an initially flat distribution for the atoms. Periodicity on the wavelength allows us to restrict the calculation to one unit cell the size of the laser wavelength, i.e., we assume periodic initial conditions [15]. Apart from these assumptions, no further approximations are made.

In Fig. 10 we show the temporal evolution of an initially delocalized ensemble of atoms. The depth of the ground state potential is chosen to get a harmonic frequency $\nu_g = 0.5\Gamma$ near the bottom of the well. The excited potential frequency is chosen as $\nu_e = \sqrt{2}\nu_g$. The Rabi frequency is $\Omega = 12\Gamma$, and the detuning of the cooling laser is $\Delta = -5\Gamma$. From Fig. 11 we see that in the present example the time scale to reach the steady state is of the order of $400\Gamma^{-1}$ which corresponds for cesium (on the $6S_{1/2} \rightarrow 6P_{3/2}$ transition) to a time of 13 μs. This demonstrates the experimental feasibility of our localization scheme. Initially delocalized atoms become localized on a time scale that agrees with the cooling rates derived from our semiclassical analysis of Sec. II.

Furthermore we have studied numerically a scheme to realize the Λ configuration used in our discussion of Raman cooling with an $F = 2 \rightarrow F' = 2$ transition. We restrict the discussion again to the final stages of cooling, i.e., we assume the atoms are already localized near the bottom of the potential well and make again a harmonic approximation. By choosing a laser configuration of two counterpropagating beams with σ^+ and σ^- polarization, respectively, and by unbalancing the Rabi frequencies of these two beams we achieve optical pumping of the atom to a Λ system formed by the states

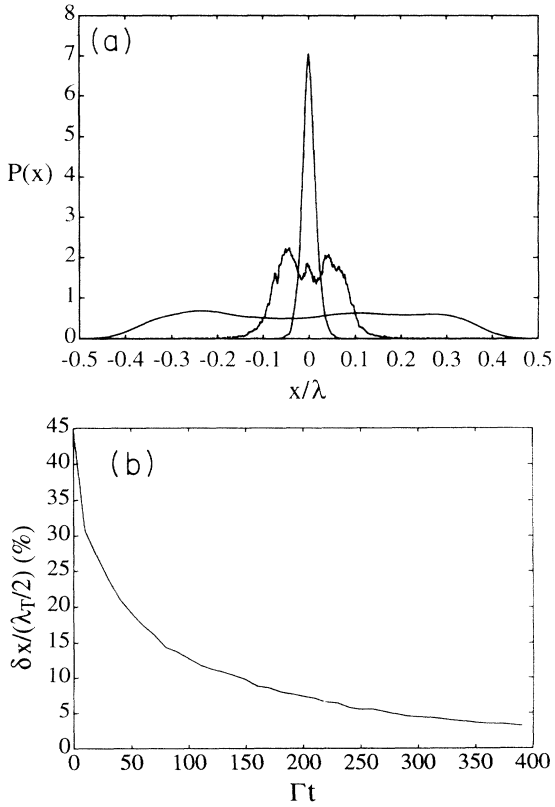

FIG. 10. Transient calculation for a two-level system in the presence of a trapping potential. The parameters are $\Omega = 12\Gamma$, $\Delta = -5\Gamma$, $\nu_g = 3\Gamma$, and $\nu_e = 2\nu_g$. (a) Position distribution for different times: initially flat distribution becomes localized; the chosen times are $t = 0, 100, 400$ in units of Γ. (b) Time evolution of the position mean square.

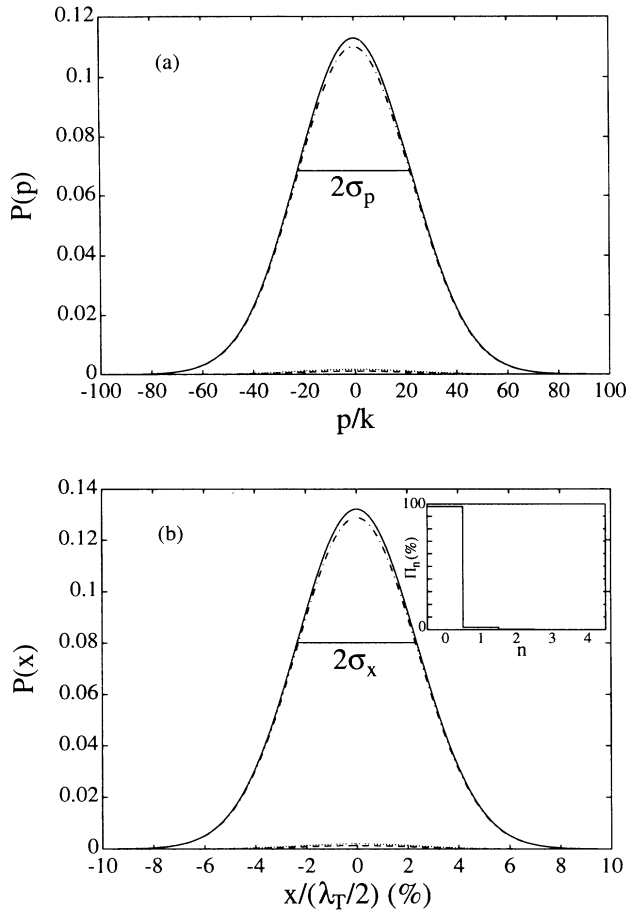

FIG. 11. Steady state momentum (a) and position (b) distribution for Raman cooling in an $F = 2 \rightarrow F' = 2$ transition. The solid line is the trace over the Zeeman sublevels, the dotted (dashed, dot-dashed) lines correspond to the distribution of the $M_F = 0$ $(+1, +2)$ states, respectively. The parameters are $\nu = \Gamma/5$, $\Delta_{23} = -10\Gamma$, $\Omega_{21} = 2.6\Gamma$, and $\Omega_{21}/\Omega_{23} = 10$. Δ_{21} is chosen to match the Raman cooling condition given by $\delta = -\nu$. The inset of (b) shows the steady state population. σ_x and σ_p correspond to the half-width at $e^{-1/2}$ of the space and momentum distribution, respectively.

$M_F = +1$, $M_{F'} = +1$, and $M_F = +2$. We expect the Raman cooling mechanisms to be valid for this situation. We again perform a quantum simulation of the corresponding master equation (7). In Fig. 11 we show steady state momentum, position, and population distributions for Raman cooling in an $F = 2 \rightarrow F' = 2$ transition. The parameters are $\nu = \Gamma/5$, $\Delta_{23} = -10\Gamma$, $\Omega_{21} = 2.6\Gamma$, and $\Omega_{21}/\Omega_{23} = 10$. Δ_{21} is chosen to match the Raman cooling condition given by $\delta = -\nu$. The agreement between the results of Sec. III and the simulation results shows that the picture of Raman cooling is valid for more general level schemes and we can expect to apply the results for cooling rates and final energies of this picture to realistic atomic configurations.

V. CONCLUSION

In this paper we have discussed cooling dynamics and localization of atoms in deep potentials induced by a far-off-resonant standing-wave laser. For a two-level atom we find that laser cooling occurs via a Sisyphus cooling mechanism which requires $\nu_g < \nu_e$ with $\nu_{g,e}$ the oscillation frequency of the atom in the trapping potential for the atom in the ground (excited) state. This corresponds to an "induced" cooling scheme with cooling times significantly faster than the cooling time scale in ion traps. Optimum localization occurs if the atoms are cooled to the vibrational ground state. This requires that the atomic oscillation frequencies are larger than the spontaneous decay width, $\nu_{g,e} > \Gamma$. Typically this can be achieved with trapping laser intensities of the order of a few MW/cm^2 [4,5]. If the trapping laser is detuned to the blue, atoms will localize near the nodes of the laser light which strongly suppresses spontaneous emissions due to excitation by the nonresonant light field. As a second scheme we have investigated Raman cooling in a three-level Λ system. For alkali atoms the two ground states are typically Zeeman levels belonging to the s state hyperfine structure manifold and in this case the optical potential for the two ground states are identical. This leads to a Raman cooling mechanism in complete analogy to ion traps.

Localization of atoms as described in this paper is interesting from the point of view of lithography with laser-manipulated atoms [16]. The cooling and trapping of neutral atoms in deep laser-induced potential wells is similar to ion traps and may be one way to realize a single-atom trap.

ACKNOWLEDGMENTS

We thank M. Lewenstein, C. Wieman, and C. Wood for discussions. J.I.C. thanks JILA for hospitality and NATO for financial support. The work at JILA was supported in part by the National Science Foundation.

APPENDIX A: BOGOLIUBOV TRANSFORM

The ladder operators a_g, a_e for the ground state and the excited state are related through a Bogoliubov transform

$$\begin{pmatrix} a_e \\ a_e^\dagger \end{pmatrix} = \begin{pmatrix} \cosh r & -\sinh r \\ -\sinh r & \cosh r \end{pmatrix} \begin{pmatrix} a_g \\ a_g^\dagger \end{pmatrix},$$

where r is given by

$$r = \operatorname{arccosh}\left(\frac{1}{2}\frac{\nu_e + \nu_g}{\sqrt{\nu_e \nu_g}}\right) \tag{A1}$$

or in terms of the squeezing operator $S(r)$,

$$a_e = S^\dagger(r) a_g S(r) \tag{A2}$$

with

$$S(r) = e^{\frac{r}{2}(a_g^2 - a_g^{\dagger 2})}. \tag{A3}$$

The number states are related through

$$|n\rangle_e = S^\dagger |n\rangle_g. \tag{A4}$$

APPENDIX B: SEMICLASSICAL FORMULAS

In Sec. III we have described qualitatively the cooling mechanism for a two-level atom confined in a superdeep potential in terms of transitions between the (cooling laser) dressed levels. In this appendix we give some analytical results for this semiclassical approach, as well as for its regime of validity.

Let us consider an atom initially in the state $|-\rangle$, oscillating in the potential $V_-(x)$ with energy E_-. After a time of the order of $\Gamma_{-,+}^{-1}$ it will be transferred to the state $|+\rangle$ at a certain position x, where it oscillates with an energy $E_+ = E_- + [V_+(x) - V_-(x)]$. Then, after a time of the order of $\Gamma_{+,-}$ and at the position x' it is transferred back to $|-\rangle$, where it oscillates with an energy $E'_- = E_+ + [V_-(x') - V_+(x')]$. The energy balance of the cycle $|-\rangle \to |+\rangle \to |-\rangle$ is

$$\begin{aligned}\delta E(x,x') &= E'_- - E_- \\ &= [V_+(x) - V_-(x)] + [V_-(x') - V_+(x')] \\ &= \sqrt{\Delta'(x)^2 + \Omega^2} - \sqrt{\Delta'(x')^2 + \Omega^2}. \end{aligned} \tag{B1}$$

The time it takes for the atom to perform this cycle is of the order of

$$\delta\tau(x,x') \sim \frac{1}{\Gamma_{-,+}(x)} + \frac{1}{\Gamma_{+,-}(x')}. \tag{B2}$$

Defining the cooling rate (in analogy with the cooling rate for ion traps) as $W = \delta E/\delta\tau/E_-$ for this cycle, and averaging over all possible x and x', we obtain

$$\frac{1}{E_-}\left\langle \frac{\delta E}{\delta\tau} \right\rangle \sim \int_{-x_-}^{x_-}\int_{-x_+}^{x_+} dx dx' P(x,x') \frac{\delta E(x,x')}{\delta\tau(x,x')}, \tag{B3}$$

where $P(x,x')$ is the probability for the atom to perform a transition from $|-\rangle$ to $|+\rangle$ at x and a subsequent transition from $|+\rangle$ to $|-\rangle$ at x', and is given by

$$\begin{aligned} P(x,x') = K^{-1} &\frac{\Gamma_{-,+}(x)}{\sqrt{\frac{2}{M}[E_- - V_-(x)]}} \\ &\times \frac{\Gamma_{+,-}(x')}{\sqrt{\frac{2}{M}[E_+(x) - V_-(x')]}}, \end{aligned} \tag{B4}$$

with K a normalization constant. In (B3), $x_\pm$ are the turning points of the potentials $V_\pm$ for the atoms with energies $E_\pm$. Note that x_+ depends on x_-, since the energy E_+ depends on the position at which the atom has made the transition from $|-\rangle$ to $|+\rangle$.

Integral (B3) can be evaluated numerically. Here, however, we will be mainly interested in the low intensity limit, where $|\Delta| > \Omega$, with $\Delta < 0$, since that is where the lowest final energies are found. In this limit, one can expand all the expressions (B1) and (B2) up to the lowest nonvanishing order in the small parameter (note $\nu_e > \nu_g$)

$$\frac{\Omega}{|\Delta| + \frac{1}{2}m(\nu_e^2 - \nu_g^2)x^2}. \tag{B5}$$

For example, we obtain

$$V_+ \simeq \frac{1}{2}m\nu_e^2 x^2 + \frac{1}{2}|\Delta|, \tag{B6a}$$

$$V_- \simeq \frac{1}{2}m\nu_g^2 x^2 - \frac{1}{2}|\Delta|, \tag{B6b}$$

$$\Gamma_+ \simeq \Gamma, \tag{B6c}$$

$$\Gamma_- \simeq \frac{1}{16}\Gamma \frac{\Omega^4}{[|\Delta| + \frac{1}{2}m(\nu_e^2 - \nu_g^2)x^2]^4}. \tag{B6d}$$

With these formulas, one can perform integral (B3) and find an analytical expression for the cooling rate. We omit this expression here since it is very involved and does not give any further information. However, from (B6) one can already see that in the low intensity limit, the cooling rate is proportional to Ω^4, i.e., the higher the Ω, the faster the cooling becomes.

So far we have not mentioned the conditions of validity of the estimation (B3). In order to derive it, apart from the semiclassical approximation, we have neglected (i) the nonsecular terms in the rate equations (20), and (ii) nonadiabatic transitions from the dressed states due to the motion of the atom in the potentials. Nonsecular terms are negligible in the limit $\Omega^2 + \Delta^2 \gg \Gamma$ (which coincides with the regime where the lowest temperatures are found). On the other hand, nonadiabatic transitions due to the atomic motion are negligible when they are less likely to occur than transitions due to the exchange of photons. Following Ref. [10] one can overestimate the probability of a nonadiabatic transfer of population during half a period of oscillation in one of the potentials by

$$P_{i,j}^{NA} \le \sup_x \frac{|v_i|^2|\theta'|^2}{\Omega^2 + \Delta'(x)^2} \qquad (i,j = \pm), \tag{B7}$$

where

$$\theta' \equiv \frac{d\theta}{dx} = -\frac{1}{2}m(\nu_e^2 - \nu_g^2)x\frac{\Omega}{\Omega^2 + \Delta'(x)^2}, \tag{B8}$$

and v_i is the atomic velocity in the state i. This probability is to be compared to the probability of a radiative transfer of population during half a period of oscillation. This latter can be estimated by

$$P_{i,j}^{x} \sim \int_{-x_{\max}^i}^{x_{\max}^i} dx \frac{\Gamma_{i,j}}{|v_i|}. \tag{B9}$$

Clearly, the higher the Rabi frequency is, the better the approximation becomes. For low intensities, one can use (B6) and substitute them in the above probabilities. The result is very similar to the one found for the optical molasses case, where in order to neglect the nonradiative transfer of populations, a rather large detuning (compared to trap frequencies and decay rates) is needed. However, when comparing the semiclassical results with the Monte Carlo wave function simulations, we have found qualitative agreement even for detunings of the same order of magnitude as the other parameters.

[1] P. Verkerk, B. Lounis, C. Salomon, C. Cohen-Tannoudji, J.Y. Courtois, and G. Grynberg, Phys. Rev. Lett. **68**, 3861 (1992); P.S. Jessen, C. Gerz, P.D. Lett, W.D. Phillips, S.L. Ralston, R.J.C. Spreeuv, and C.I. Westbrook, *ibid.* **69**, 49 (1992).

[2] P. Marte, R. Dum, R. Taieb, P. Lett, and P. Zoller, Phys. Rev. Lett. **71**, 1335 (1993).

[3] J.Y. Courtois and G. Grynberg, Phys. Rev. A **46**, 7060 (1992).

[4] J.D. Miller, R.A. Cline, and D. Heinzen, Phys. Rev A **47**, R4567 (1993).

[5] For example, for cesium choosing a laser with a wavelength λ_T=877 nm (e.g., a Ti-sapphire laser) we get for the dynamic atomic polarizabilities $\alpha_g = 767$ MHz/(MW/cm^2) and $\alpha_e = 1508$ MHz/(MW/cm^2). To obtain a harmonic frequency at the bottom of the potential which is equal to the radiative decay width, $\nu_g = \Gamma$, an intensity of 4.2 MW/cm^2 is required (the corresponding ν_e is $\nu_e = \sqrt{\alpha_e/\alpha_g}\Gamma$). For this intensity the scattering rate of nonresonant photons would then be of the order of a few tens per second.

[6] S. Stenholm, Rev. Mod. Phys. **58**, 699 (1986).

[7] See, for example, D.J. Wineland, W.M. Itano, and R.S. VanDyck, J. Adv. At. Mol. Phys. **19**, 135 (1983); R. Blatt, in *Fundamental Systems in Quantum Optics*, Proceedings of the Les Houches Summer School, Session LIII, edited by J. Dalibard, J.M. Raymond, and J. Zinn-Justin (Elsevier, Amsterdam, 1992), p. 253.

[8] M. Lindberg and J. Javanainen, J. Opt. Soc. Am. B **3**, 1008 (1986).

[9] A.P. Kazantsev, G.I. Surdutovich, and V.P. Yakovlev, *Mechanical Action of Light on Atoms* (World Scientific, Singapore, 1990).

[10] J. Dalibard and C. Cohen-Tannoudji, J. Opt. Soc. Am. B **6**, 2023 (1989); J. Dalibard and C. Cohen-Tannoudji, J. Opt. Soc. Am. B **2**, 1707 (1985).

[11] We note that the conditions for adiabatic elimination is based on a low intensity assumption. This is different from the adiabatic elimination in the case of ion traps which is valid for small Lamb-Dicke parameter (but arbitrary intensities); see [8,13].

[12] I.I. Sobel'man, *Introduction to the Theory of Atomic Spectra* (Pergamon Press, Oxford, 1972).

[13] J.I. Cirac, R. Blatt, P. Zoller, and W.D. Phillips, Phys. Rev. A **46**, 2668 (1992).

[14] R. Dum, P. Zoller, and H. Ritsch, Phys. Rev. A **45**, 4879 (1992); J. Dalibard, Y. Castin, and K. Molmer, Phys. Rev. Lett. **68**, 580 (1992); H. Carmichael, *An Open Systems Approach to Quantum Optics* (Springer Verlag, New York, 1993).

[15] P. Marte, R. Dum, R. Taieb, and P. Zoller, Phys. Rev. A **47**, 1378 (1993).

[16] G. Timp, R.E. Behringer, D.M. Tennant, J.E. Cunningham, M. Prentiss, and K.K. Berggren, Phys. Rev. Lett. **69**, 1636 (1992); J. McClelland, R.E. Scholten, E.C. Palm, and R.J. Celota, Science **262**, 877 (1993).